



Article

New Pyrroline Isolated from Antarctic Krill-Derived Actinomycetes *Nocardiopsis* sp. LX-1 Combining with Molecular Networking

Ting Shi ^{1,2} , Yan-Jing Li ¹, Ze-Min Wang ², Yi-Fei Wang ¹, Bo Wang ^{1,*}  and Da-Yong Shi ^{2,*} ¹ College of Chemical and Biological Engineering, Shandong University of Science and Technology, Qingdao 266590, China² State Key Laboratory of Microbial Technology, Institute of Microbial Technology, Shandong University, Qingdao 266237, China

* Correspondence: wb@sdu.edu.cn (B.W.); shidayong@sdu.edu.cn (D.-Y.S.)

Abstract: Antarctic krill (*Euphausia superba*) of the *Euphausiidae* family comprise one of the largest biomasses in the world and play a key role in the Antarctic marine ecosystem. However, the study of *E. superba*-derived microbes and their secondary metabolites has been limited. Chemical investigation of the secondary metabolites of the actinomycetes *Nocardiopsis* sp. LX-1 (in the family of *Nocardiopsaceae*), isolated from *E. superba*, combined with molecular networking, led to the identification of 16 compounds **a–p** (purple nodes in the molecular network) and the isolation of one new pyrroline, nocardpyrroline A (**1**), along with 11 known compounds **2–12**. The structure of the new compound **1** was elucidated by extensive spectroscopic investigation. Compound **2** exhibited broad-spectrum antibacterial activities against *A. hydrophila*, *D. chrysanthemi*, *C. terrigena*, *X. citri* *pv. malvacearum* and antifungal activity against *C. albicans* in a conventional broth dilution assay. The positive control was ciprofloxacin with the MIC values of <0.024 μ M, 0.39 μ M, 0.39 μ M, 0.39 μ M, and 0.20 μ M, respectively. Compound **1** and compounds **7**, **10**, and **11** displayed antifungal activities against *F. fujikuroi* and *D. citri*, respectively, in modified agar diffusion test. Prochloraz was used as positive control and showed the inhibition zone radius of 17 mm and 15 mm against *F. fujikuroi* and *D. citri*, respectively. All the annotated compounds **a–p** by molecular networking were first discovered from the genus *Nocardiopsis*. Nocardpyrroline A (**1**) features an unprecedented 4,5-dihydro-pyrrole-2-carbonitrile substructure, and it is the first pyrroline isolated from the genus *Nocardiopsis*. This study further demonstrated the guiding significance of molecular networking in the research of microbial secondary metabolites.

Keywords: molecular networking; Antarctic krill; *Nocardiopsis* sp. LX-1; pyrroline; nocardpyrroline A; antimicrobial activity



Citation: Shi, T.; Li, Y.-J.; Wang, Z.-M.; Wang, Y.-F.; Wang, B.; Shi, D.-Y. New Pyrroline Isolated from Antarctic Krill-Derived Actinomycetes *Nocardiopsis* sp. LX-1 Combining with Molecular Networking. *Mar. Drugs* **2023**, *21*, 127. <https://doi.org/10.3390/md21020127>

Academic Editors: Roberta Teta and Giuseppina Chianese

Received: 30 November 2022

Revised: 10 February 2023

Accepted: 14 February 2023

Published: 15 February 2023



Copyright: © 2023 by the authors. Licensee MDPI, Basel, Switzerland. This article is an open access article distributed under the terms and conditions of the Creative Commons Attribution (CC BY) license (<https://creativecommons.org/licenses/by/4.0/>).

1. Introduction

The extreme environments of Antarctica, including severe cold, an arid climate, and solar radiation, have created a unique ecological system. Creatures in the Antarctic ecosystem, in particular microorganisms, usually have to produce some structurally specific active substances to adapt to the harsh conditions [1]. Antarctic krill (*Euphausia superba*), a small crustacean in the family of *Euphausiidae* in the Antarctic Ocean, with one of the largest biomasses (approximately 379 million metric tons) in the world, plays a key role in the Antarctic marine ecosystem [2]. Antarctic krill is critical in the food chain for seals, whales, and penguins, making it the foundation of the Southern Ocean ecosystem and an important marine living resource [3,4]. The research on Antarctic krill has mainly focused on its fisheries [5], nutritive value [6], and distribution [7]. To the best of our knowledge, only three studies have focused on Antarctic krill-derived microbes and their secondary

metabolites [8–10], so there is great potential to discover new bioactive natural products from *Euphausia superba* symbiotic microorganisms.

The genus *Nocardiopsis* is one of the important actinomycetes for its widespread application in industry [11], agriculture [12], and environmental protection [13], and especially for its ability to produce a wide variety of new compounds with different skeletons and diverse biological activities [14–16]. The bioactive compounds produced by *Nocardiopsis* can assist it to survive under different and hostile environmental conditions, even in the Antarctic marine ecosystem [14,17].

Molecular networking has been an excellent methodology by which to visualize and annotate the secondary metabolites of fungi crude extracts based on nontargeted tandem mass (MS/MS) data in the Global Natural Products Social Molecular Networking (GNPS; <http://gnps.ucsd.edu>) platform [18–20]. Molecular networking has become an efficient way to dereplicate mixtures and discover new natural products [21]. In our ongoing research of secondary metabolites produced by Antarctic microorganisms, some new bioactive compounds have been found with molecular networking [22,23].

Antimicrobial resistance (AMR) has become an increasing problem with the misuse and overuse of antibiotics, causing infections increasingly difficult or impossible to treat with existing drugs [24–26]. The WHO has declared AMR to be one of the top 10 global public health threats. Antibiotic shortages are affecting countries in all regions. A lack of access to quality antimicrobials also remains a major issue [27]. Natural products from microorganisms have played a significant role in delivering antibiotics since the discovery of penicillin in the 1940s [28].

Chemical investigation of the fermentation broth of crude extracts of the actinomycetes *Nocardiopsis* sp. LX-1, derived from the Antarctic krill *E. superba*, has been carried out to find more antimicrobial compounds. The antimicrobial activity of the crude extracts against *Candida albicans* showed an inhibition rate of $70 \pm 0.46\%$ at the concentration of 100 $\mu\text{g/mL}$, combined with molecular networking. In this report, the compounds recognized by molecular networking and the isolation, structure elucidation, and antimicrobial activity evaluation of the isolated compounds are discussed.

2. Results and Discussion

2.1. Visualized Secondary Metabolic Profile and Identified Compounds by Molecular Networking

The actinomycetes *Nocardiopsis* sp. LX-1 was cultured in nutrient broth (NB) and extracted by EtOAc repeatedly to obtain organic crude extracts. Then, the crude extract samples were diluted and subjected to UHPLC-MS/MS analysis to obtain the raw MS/MS data. The obtained MS/MS data were converted into .mzXML format and uploaded to the GNPS platform to obtain the molecular network (Figure 1, <https://gnps.ucsd.edu/ProteoSAFe/status.jsp?task=37dd96194c924f6d9daee62672ba930>, accessed on 29 November 2021) of the secondary metabolic profile of the actinomycetes *Nocardiopsis* sp. LX-1. This was finally visualized by Cytoscape software. The molecular network of the metabolic profile of LX-1 contained 473 nodes and 530 edges, meaning there were 473 compounds annotated by molecular networking in the raw MS/MS data of the actinomycetes crude extracts. The compounds that shared similar MS/MS fragments and similar chemical structures were connected by edges and clustered together into a molecular family. There were 31 molecular clusters (over two nodes) in the LX-1 molecular network, and the maximal cluster contained 33 nodes, meaning 33 compounds with similar chemical structures were in the first molecular cluster (Figure 1). The purple nodes in Figure 1 express compounds annotated by molecular networking and blue nodes mean compounds not identified by molecular networking. Most of the compounds (blue nodes) in the molecular network were unknown after searching in the GNPS database (Figure 1), indicating the crude extracts produced by *Nocardiopsis* sp. LX-1 might possess abundant new compounds.

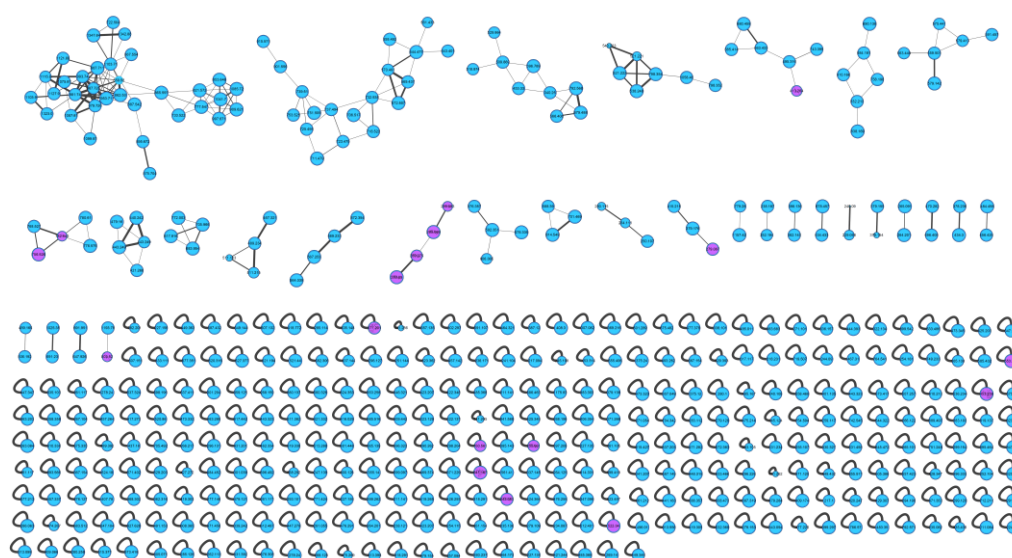


Figure 1. Molecular network of the actinomycetes *Nocardioopsis* sp. LX-1. The purple nodes are compounds annotated by molecular networking and blue nodes are compounds not identified by molecular networking. The numbers in nodes mean precursor mass of compounds. The size of the nodes decided by precursor intensity represents the quantity of the compounds.

The molecular networking was used to preliminarily investigate the number and the structural types of the secondary metabolites of the actinomycetes *Nocardioopsis* sp. LX-1 and predicted the possibility of finding new compounds to determine the research value of the actinomycetes. After analysis by molecular networking, 16 compounds **a–p** (purple nodes) (Figures 2 and 3, Table 1) were characterized from the crude extracts of *Nocardioopsis* sp. LX-1 by comparing their MS/MS spectra with those in the GNPS library. The plastic products were avoided during the extraction and purification, and the plasticizers **i** and **j** might be contaminated by the organic extracted solvent, which were not the LC-MS grade/HPLC grade solvents that might contain contaminants. All the compounds **a–p**, identified by molecular networking, were preliminarily detected from the crude extracts of *Nocardioopsis* sp. LX-1. The big cluster families of the LX-1 molecular network with heavy molecular weight are speculated to be fatty acid compounds which could be lost in separated process. A series of antimicrobial isoflavonoids and flavonoids (**a–f**) were identified by molecular networking, which should be the target natural products to be isolated from LX-1. None of the recognized compounds **a–p** had been isolated from the genus *Nocardioopsis* until now, indicating the ability of molecular networking to analyze microbial secondary metabolites and guide the directional separation.

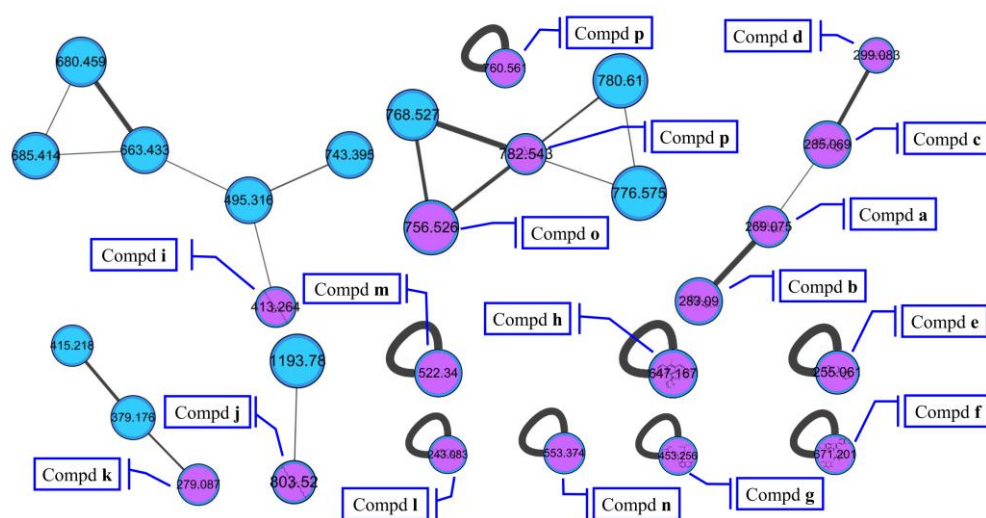


Figure 2. Compounds **a–p** identified by molecular networking from *Nocardiosis* sp. LX-1. The purple nodes are compounds annotated by molecular networking and blue nodes are compounds not identified by molecular networking. The numbers in nodes mean precursor mass of compounds. The letters **a–p** in bold format represent different recognized compounds. The size of the nodes decided by precursor intensity represents the quantity of the compounds.

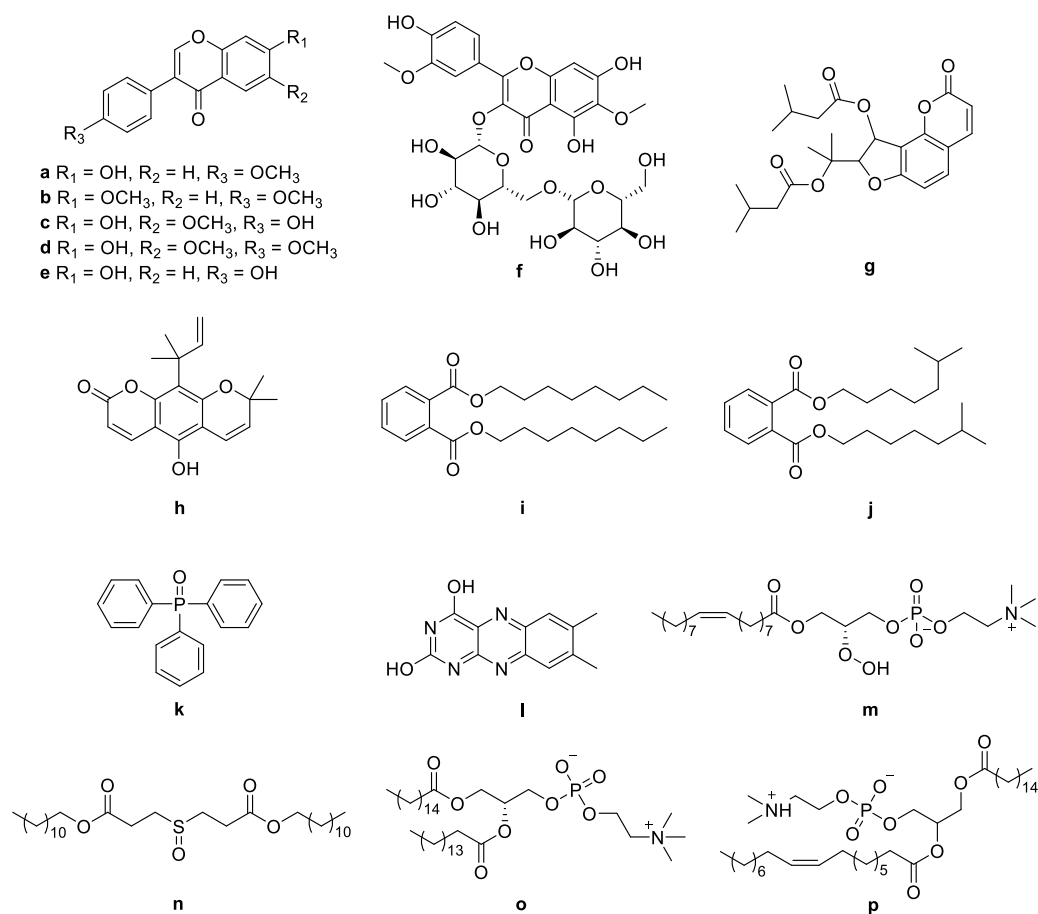


Figure 3. Chemical structures of **a–p** identified by molecular networking from *Nocardiosis* sp. LX-1.

Table 1. Compounds **a–p** identified by molecular networking from *Nocardiopsis* sp. LX-1.

No.	Name	Adduct	Precursor Mass	Exact Mass	CAS Number	RT (min)	Molecular Formula	Class
a	Formonentin	[M + H] ⁺	269.075	268.074	485723	45.6	C ₁₆ H ₁₂ O ₄	Isoflavonoids
b	Dimethoxydaidzein	[M + H] ⁺	283.090	282.089	1157397	49.1	C ₁₇ H ₁₄ O ₄	Isoflavonoids
c	Glycitein	[M + H] ⁺	285.069	284.068	40957833	39.9	C ₁₆ H ₁₂ O ₅	Isoflavonoids
d	Afrormosin	[M + H] ⁺	299.083	298.29	550798	46.5	C ₁₇ H ₁₄ O ₅	Isoflavonoids
e	Daidzein	[M + H] ⁺	255.061	254.058	486668	38.9	C ₁₅ H ₁₀ O ₄	Isoflavonoids
f	Spinacetin	[M + H] ⁺	671.201	670.175	101021298	64.0	C ₂₉ H ₃₄ O ₁₈	Flavonoids
g	3-O-β-gentiobioside Athamantin (6Cl,7Cl)	[M + Na] ⁺	453.256	430.49	1892564	39.1	C ₂₄ H ₃₀ O ₇	Coumarin derivatives
h	Nordentatin	[2M + Na] ⁺	647.167	312.137	1083193150	64.0	C ₁₉ H ₂₀ O ₄	Coumarin derivatives
i	Diioctyl phthalate	[M + Na] ⁺	413.264	390.277	117840	63.8	C ₂₄ H ₃₈ O ₄	Benzene derivatives
j	Diisooctyl phthalate	[2M + Na] ⁺	803.520	390.277	131204	63.7	C ₂₄ H ₃₈ O ₄	Benzene derivatives
k	Triphenylphosphine oxide	[M + H] ⁺	279.087	278.28	791286	45.3	C ₁₅ H ₁₅ OP	Benzene derivatives
l	Lumichrome	[M + H] ⁺	243.083	242.238	1086802	22.7	C ₁₂ H ₁₀ N ₄ O ₂	Pteridine derivatives
m	1-(9Z- Octadecenoyl)-sn- glycero-3- phosphocholine	[M + H − O] ⁺	522.340	537.667	19420565	65.5	C ₂₆ H ₅₂ NO ₈ P	Lipids
n	Didodecyl 3,3'- sulfinyldipropionate	[M + Na] ⁺	553.374	530.844	17243140	67.2	C ₃₀ H ₅₈ O ₅ S	Lipids
o	1,2-Dipalmitoyl-L- lecithin	[M + Na] ⁺	756.526	734.039	63898	75.9	C ₄₀ H ₈₀ NO ₈ P	Lipids
p	1-Palmitoyl-2-oleoyl- L-α-lecithin	[M + H] ⁺ [M + Na] ⁺	760.561 782.543	759.578	26853316	63.8	C ₄₂ H ₈₂ NO ₈ P	Lipids

2.2. Structure Elucidation and Antimicrobial Activity of Isolated Compounds 1–12

Chemical investigation of the broth fermentative crude extracts of *Nocardiopsis* sp. LX-1 was carried out to find the molecular networking analyzed compounds, and led to the isolation of one new compound, nocarpyrroline A (**1**), along with 11 known compounds **2–12** (Figure 4). However, only one target flavonoid derivative, daidzein (**2**, same as the molecular networking identified isoflavonoid **e**), in the molecular network was isolated, which might be due to the insufficient fermentation of *Nocardiopsis* sp. LX-1 and its low yield of the isoflavonoid and flavonoid compounds. This is the first time isoflavonoid has been isolated from the genus *Nocardiopsis*. Compounds **1**, **2**, and **4–8** were appeared in the molecular network of *Nocardiopsis* sp. LX-1 as individual nodes (Figure 5). The self-loops of compounds **1** and **2** in the network might because their MS/MS spectra are not informative due to the low amount of the compounds; therefore no peak matches with other clustered nodes. Compounds **4–8** were appeared as individual nodes might be due to the fact that cyclic dipeptides are harder to be ionized in the positive ESI MS/MS experiment than in the negative ESI MS/MS experiment. Compound **9** was not detected in ESI⁺ MS/MS spectra of *Nocardiopsis* sp. LX-1 because it cannot ionize in positive MS/MS measurement. Compounds **8** and **10–12** were not found in the molecular network might be due to their low molecular weight, which is hard to be detect.

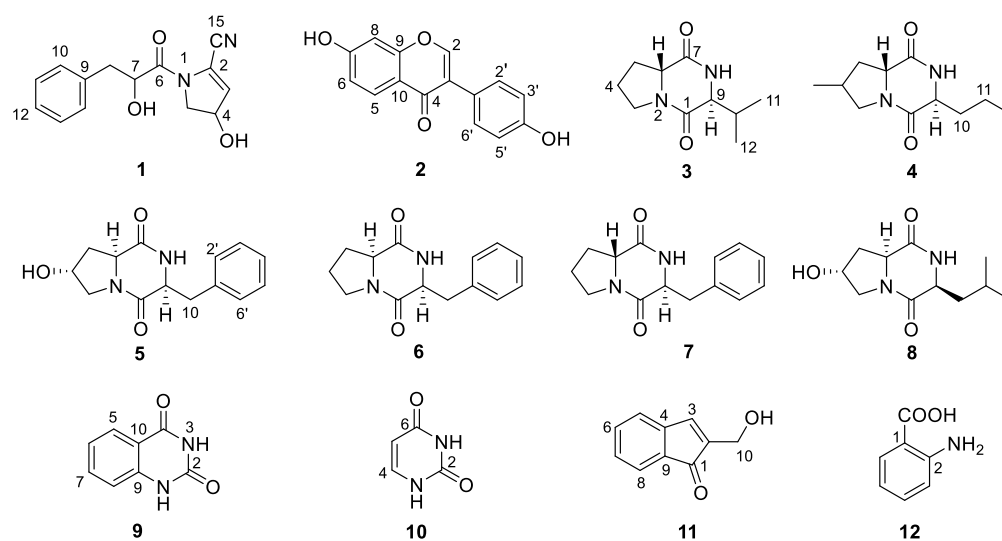


Figure 4. Compounds 1–12 isolated from *Nocardioopsis* sp. LX-1.

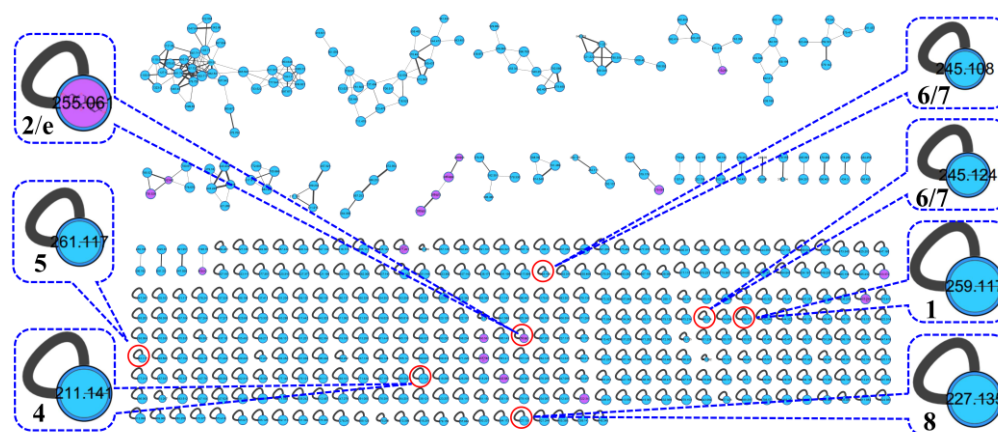


Figure 5. Isolated compounds in the molecular network of *Nocardioopsis* sp. LX-1. The size of the nodes decided by precursor intensity represents the quantity of the compounds.

Nocarpyrroline A (1) was obtained as an amorphous white powder. Its molecular formula was determined as $C_{14}H_{14}O_3N_2$ by HR-ESI-MS with the $[M-H]^-$ peak at m/z 257.0939 (calculated for $C_{14}H_{13}O_3N_2$, 257.0932) (Figure S7) and $[M+H]^+$ peak at m/z 259.1080 (calculated for $C_{14}H_{15}O_3N_2$, 259.1077) (Figure S8), containing nine degrees of unsaturation. The five aromatic proton signals at δ_H 7.09–7.04 (1H, m), 7.24–7.20 (1H, m), 7.20–7.17 (1H, m), 7.24–7.20 (1H, m), and 7.09–7.04 (1H, m) in 1H NMR data of 1 (Table 2 and Figure S1), combined with the six ^{13}C NMR signals at δ_C 135.6 C, 131.0 CH, 129.3 CH, 128.2 CH, 129.3 CH, 131.0 CH (Table 2 and Figure S2), indicated that there was a phenyl group in 1. The HMBC correlations from H-8 to C-9/C-10/C-14 proved the phenyl group was linked at C-8 (Figure 6). The 1H NMR, ^{13}C NMR, HSQC and HR-ESI-MS spectra (Figures S1–S3 and Figure S7) of 1 displayed one unsaturated quaternary carbon at δ_C 135.2, one unsaturated methine at δ_H 5.73 (1H, d, 2.7 Hz), δ_C 119.6, one oxygenated methine at δ_H 4.71 (1H, ddd, 8.2, 3.5, 2.7 Hz), δ_C 70.2, and one methylene at δ_H 3.72 (1H, dd, 13.6, 8.2 Hz), 3.62 (1H, dd, 13.6, 3.5 Hz), and δ_C 54.5, demonstrated a pyrroline ring with a hydroxyl substituent group in 1. The COSY cross-peaks of H-3/H-4 and H-4/H-5, and the HMBC correlations from H-3 to C-2 and H-3 to C-5 further proved the existence of a pyrroline ring in 1 (Figure 6). One unsaturated quaternary carbon at δ_C 164.2 showed there was a carbonyl group in 1. The HMBC correlation between H-8 and C-6, and the COSY cross peak of H-7/H-8, revealed the carbonyl group was in the location of C-6 (Figure 6). The high field shift of the C-6 carbonyl group indicated the amide linkage between C-6 and N-1

(Table 2). The IR absorption band at 2253 cm^{-1} (Figure S9), combined with the molecular formula of $\text{C}_{14}\text{H}_{14}\text{O}_3\text{N}_2$ and the nine degrees of unsaturation suggested that there was one cyano group in **1**. The high field shift of C-2 and low field shift of C-3 indicated that the cyano group was linked at C-2 (Table 2). Thus, the plane structure of **1** was established unambiguously as shown in Figure 4. The NOESY spectrum was measured to determine the relative configuration of **1**; however, the NOESY cross-peaks were not clear enough to identify the relative configuration of **1**. The absolute configuration of **1** was attempted to determine by the modified Mosher's method. Unfortunately, it was failed due to the limited quantity of **1**.

Table 2. NMR spectroscopic data (400/100 MHz) of nocarpyrroline A (**1**) in methanol- d_4 .

Position	δ_{C}	δ_{H} (J in Hz)
2	135.2, C	
3	119.6, CH	5.73, d (2.7)
4	70.2, CH	4.71, ddd (8.2, 3.5, 2.7)
5	54.5, CH_2	3.72, dd (13.6, 8.2); 3.62, dd (13.6, 3.5)
6	164.2, C	
7	59.1, CH	4.48, t (4.0)
8	41.1, CH_2	3.24, d (3.8); 2.96, dd (13.6, 4.5)
9	135.6, C	
10	131.0, CH	7.09–7.04, m
11	129.3, CH	7.24–7.20, m
12	128.2, CH	7.20–7.17, m
13	129.3, CH	7.24–7.20, m
14	131.0, CH	7.09–7.04, m
15	119.7, C	

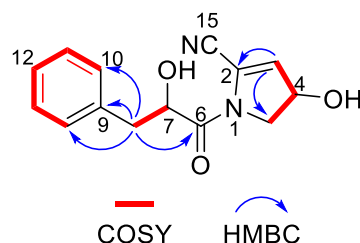


Figure 6. Key COSY and HMBC correlations of nocarpyrroline A (**1**).

The new compound nocarpyrroline A (**1**) was proposed to be biosynthesized by the condensation reaction of hydroxyl-cinnamate and 4-hydroxy-4,5-dihydro-1H-pyrrole-2-carbonitrile (Figure 7). Hydroxyl-cinnamate was suggested to be obtained from the hydroxylation of cinnamate. Phenyllactic acid (PLA) was biosynthesized from phosphoenolpyruvate and erythrose-4-phosphate through the enzymes of 3-deoxy-7-phosphoheptulonate synthase (DAHPS), 3-dehydroquinic acid synthase (DHQS), 3-dehydroquinic acid dehydratase (DHQD), shikimic acid 5-dehydrogenase (SDH), shikimic acid kinase (SK), 3-enolpyruvylshikimic acid 5-phosphate synthase (EPS), chorismic acid synthase (CS), chorismic acid mutase (CM), prephenic acid aminotransferase (PAT), arogenic acid dehydratase (ADT), aminotransferase (ATF), dehydrogenase (DHG) in sequence [29,30]. Then, 4-hydroxy-4,5-dihydro-1H-pyrrole-2-carbonitrile was deduced to be achieved through amination, dehydration, hydroxylation, and reduction of L-Pro. L-Pro was biosynthesized from L-glutamate- γ -semialdehyde catalyzed by Δ^1 -pyrroline-5-carboxylate reductase. L-glutamate- γ -semialdehyde could be acquired by Δ^1 -pyrroline-5-carboxylate synthase from L-Glu or received through catalyzing L-ornithine by ornithine- δ -aminotransferase (Figure 7) [31].

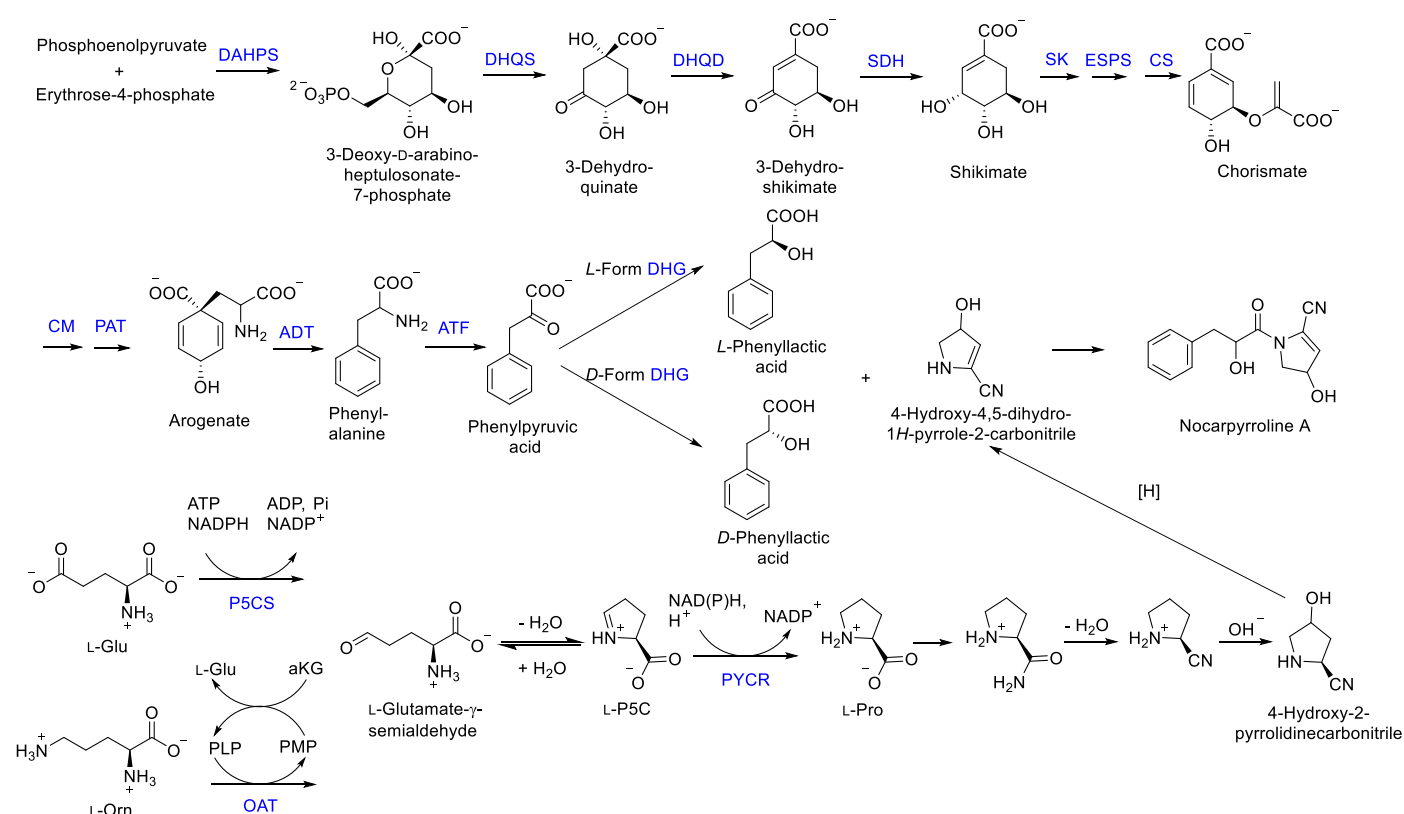


Figure 7. Plausible biogenetic pathway proposed for compound **1** [29–31]. DAHPS, 3-deoxy-7-phosphoheptulonate synthase; DHQD, 3-dehydroquinic acid dehydratase; DHQS, 3-dehydroquinic acid synthase; SDH, shikimic acid 5-dehydrogenase; SK, shikimic acid kinase; ESPS, 3-enolpyruvylshikimic acid 5-phosphate synthase; CS, chorismic acid synthase; CM, chorismic acid mutase; PAT, prephenic acid aminotransferase; ADT, arogenic acid dehydratase; ATF, aminotransferase; DHG, dehydrogenase; P5CS, Δ^1 -pyrroline-5-carboxylate synthase; OAT, ornithine- δ -aminotransferase; PYCR, Δ^1 -pyrroline-5-carboxylate reductase.

According to the plausible biogenetic pathway proposed for **1** (Figure 7), the 4-OH was deduced to be the *R* configuration to avoid steric hindrance. There were 75 conformers of **1-4R,7S** with the minimum energy of 322.98 kJ/mol and 79 conformers of **1-4R,7R** with the minimum energy of 326.88 kJ/mol through molecular mechanics MMFF method, so compound **1** tend to be **4R,7S** with lower energy. The phenyllactic acid (PLA) part of **1** can be biosynthesized as *L*-PLA by *L*-form dehydrogenase (DHG) or as *R*-PLA by *R*-form DHG (Figure 7) [29]. PLA has been found to exhibit antimicrobial activities including a range of Gram-positive bacteria, Gram-negative bacteria, yeasts and mould species [29]. Compared with **1**, only two compounds—phenylmethyl 1-acetyl-4,5-dihydro-4-hydroxy-1H-pyrrole-2-carboxylate (CAS number: 2293990-67-5) [32] and 1-(2,3-dihydro-3,3,5-trimethyl-1H-pyrrol-1-yl)-2-phenoxyethanone (CAS number: 118428-79-8) [33]—show structural similarity with over 80% searched in SciFinder, and both of the compounds were obtained through chemical synthesis. Compound **1** appeared alone in the molecular network of *Nocardiopsis* sp. LX-1 (Figure 5), indicating there is no compound showing enough MS/MS similarity with the single node in this certain sample.

Compound **2** was obtained as an amorphous white powder. Its molecular formula was determined as $C_{15}H_{10}O_4$ by HR-ESI-MS with the $[M - H]^-$ peak at m/z 253.0501 (calculated for $C_{15}H_9O_4$, 253.0506) (Figure S12) and $[M + H]^+$ peak at m/z 255.0660 (calculated for $C_{15}H_{11}O_4$, 255.0652) (Figure S13). The 15 unsaturated carbon signals at δ_C 152.4, 123.3, 174.6, 127.0, 115.0, 158.9, 102.0, 158.0, 116.5, 122.9, 130.1, 115.0, 157.0, 115.0 and 130.1, as well as eight unsaturated hydrogen signals at δ_H 8.20 (1H, s), 7.87 (1H, d, 8.8), 6.82 (1H, dd, 8.8, 2.2), 6.69 (1H, d, 2.2), 7.36 (1H, d, 8.6), 6.79 (1H, d, 8.6), 6.79 (1H, d, 8.6), and 7.36

(1H, d, 8.6) indicated that **2** was an isoflavonoid. Compound **2** was further determined as daidzene for its nearly identical ¹H NMR and ¹³C NMR data (Table S1), as compared to examples in the literature [34].

Compound **3** was obtained as an amorphous white powder. The HR-ESI-MS spectra (Figures S16 and S17) of **3** exhibited its molecular formula as C₁₀H₁₆O₂N₂ with the [M – H][–] peak at *m/z* 195.1130 (calculated for C₁₀H₁₅O₂N₂, 195.1139) and [M + H]⁺ peak at *m/z* 197.1294 (calculated for C₁₀H₁₇O₂N₂, 197.1285). The two amido-carbonyl signals at δ_C 169.9 and 165.5, and two amino-methine signals at δ_H 4.07, dd (10.1, 5.6), δ_C 58.4 and δ_H 3.70–3.62, m, δ_C 63.5 in NMR data proved that compound **3** was a diketopiperazine (DKP) (Tables S2 and S3). Further analysis showed that the ¹H NMR, ¹³C NMR, and specific optical rotation (OR) data (Tables S2–S4) of **3** demonstrated that **3** was cyclo(D-Pro-L-Val) [35].

Compound **4** was acquired as an amorphous white powder. Its molecular formula was decided by HR-ESI-MS spectra (Figures S20 and S21) as C₁₁H₁₈O₂N₂ with the [M – H][–] peak at *m/z* 209.1288 (calculated for C₁₁H₁₇O₂N₂, 209.1296) and [M + H]⁺ peak at *m/z* 211.1449 (calculated for C₁₁H₁₉O₂N₂, 211.1441), which was similar with those of **3**. It was deduced that **4** was a DKP compound similar to **3**. This deduction was further confirmed by the fact that the NMR data of **4** displayed two amido-carbonyl signals at δ_C 169.8 and 165.5, and two amino-methine signals at δ_H 4.07, dd (9.9, 6.4), δ_C 58.5 and δ_H 3.77, dd (5.7, 3.9), δ_C 62.9 (Tables S2 and S3). Compound **4** was finally proved to be cyclo(4-methyl-D-Pro-L-Nva) (**4**). Its ¹H NMR, ¹³C NMR, and specific OR data (Tables S2–S4) are almost identical to examples in the literature [36].

Compound **5** was isolated as a colorless oil. The molecular formula of **5** was ascertained as C₁₄H₁₆O₃N₂ through HR-ESI-MS spectra (Figures S24 and S25) with the [M – H][–] peak at *m/z* 259.1083 (calculated for C₁₄H₁₅O₃N₂, 259.1088), and [M + H]⁺ peak at *m/z* 261.1244 (calculated for C₁₄H₁₇O₃N₂, 261.1234) and 283.1063 (calculated for C₁₄H₁₆O₃N₂Na, 283.1053). The NMR spectra data of two amido-carbonyl signals at δ_C 166.9 and 171.0, and two amino-methine signals at δ_H 4.33, ddd (11.8, 5.9, 2.0), δ_C 58.1 and δ_H 4.45, td (5.1, 1.8), δ_C 57.4 (Tables S2 and S3) illustrated that **5** was a DKP compound. Further analysis of the ¹H NMR, ¹³C NMR, and specific OR data (Tables S2–S4) of **5** proved that **5** was cyclo(*trans*-4-OH-L-Pro-L-Phe) [37].

Compound **6** was obtained as a colorless oil. Its molecular formula was determined as C₁₄H₁₆O₂N₂ through HR-ESI-MS spectra (Figures S28 and S29) with the [M – H][–] peak at *m/z* 243.1133 (calculated for C₁₄H₁₅O₂N₂, 243.1139), and [M + H]⁺ peak at *m/z* 245.1294 (calculated for C₁₄H₁₇O₂N₂, 245.1285). The only obvious difference between the NMR data of **6** and **5** was the methylene at C-4 in **6** was substituted by hydroxy-methine in **5**. We carefully compared the NMR and specific OR data of **6** (Tables S2–S4) with those in the literature [38] and came to the determination that **6** is cyclo(L-Pro-L-Phe).

Compound **7** was acquired as a colorless oil. The HR-ESI-MS spectra (Figures S32 and S33) of **7** exhibited the same molecular formula as **6**, with the [M – H][–] peak at *m/z* 243.1133 (calculated for C₁₄H₁₅O₂N₂, 243.1139), and [M + H]⁺ peak at *m/z* 245.1293 (calculated for C₁₄H₁₇O₂N₂, 245.1285) and 267.1112 (calculated for C₁₄H₁₆O₂N₂Na, 267.1104). The NMR and specific OR data (Tables S2–S4) determined that **7** was cyclo(D-Pro-L-Phe), according to the literature [39].

Compound **8** was obtained as an amorphous white powder. The molecular formula of C₁₁H₁₈O₃N₂ was determined by HR-ESI-MS with the [M – H][–] peak at *m/z* 225.1238 (calculated for C₁₁H₁₇O₃N₂, 225.1245), and [M + H]⁺ peak at *m/z* 227.1398 (calculated for C₁₁H₁₉O₃N₂, 227.1390) and 249.1217 (calculated for C₁₁H₁₈O₃N₂Na, 249.1210) which was similar to those of **4**. We deduced that **8** was a DKP compound similar to **4**. This deduction was further confirmed by the NMR data of **8**, which displayed two amido-carbonyl signals at δ_C 168.8 and 172.9, and two amino-methine signals at δ_H 4.50, ddd (11.2, 6.5, 1.6), δ_C 58.5 and δ_H 4.15, ddd (6.6, 4.4, 1.8), δ_C 54.9 (Tables S2 and S3). Compound **8** was finally determined to be cyclo(4-hydroxyl-L-Pro-L-Leu) because it has almost the same ¹H NMR, ¹³C NMR, and specific OR data (Tables S2–S4) as examples in the literature [40].

Compound **9** was obtained as an amorphous white powder. Its molecular formula was determined to be $C_8H_6O_2N_2$ by HR-ESI-MS (Figure S40) with the $[M - H]^-$ peak at m/z 161.0345 (calculated for $C_8H_5O_2N_2$, 161.0357). The 1H NMR and ^{13}C NMR spectra of **9** exhibited eight unsaturated carbon signals at δ_C 151.0, 163.5, 127.5, 122.7, 135.4, 116.0, 141.8, and 114.9, and four aromatic-hydrogen signals at δ_H 7.87 (1H, dd, 8.3, 1.6), 7.17–7.13 (2H, m), and 7.62 (1H, ddd, 8.5, 7.3, 1.6) (Table S5), which were the NMR characteristic of quinazolinone and almost same as those in the literature [41], so **9** was identified as 2,4(1H, 3H)quinazolinone.

Compound **10** was acquired in the form of colorless needles. The HR-ESI-MS (Figures S43 and S44) of **10** showed the molecular formula as $C_4H_4O_2N_2$ with the $[M - H]^-$ peak at m/z 111.0187 (calculated for $C_4H_3O_2N_2$, 111.0200), and $[M + H]^+$ peak at m/z 113.0351 (calculated for $C_4H_5O_2N_2$, 113.0346). The two aromatic quaternary carbon signals at δ_C 151.6 and 164.4, two aromatic methine signals at δ_H 5.44, dd (7.4, 1.9), δ_C 100.3 and δ_H 7.39, dd (7.4, 5.6), δ_C 142.3, and two hydrogen bond signals at 10.83, br s and 11.03, br s in NMR data (Table S5) determined **10** to be uracil [42].

Compound **11** was obtained as a pale yellow powder. The molecular formula of $C_{10}H_8O_2$ was determined by HR-APCI-MS (Figure S47) with the $[M + H]^+$ peak at m/z 161.0602 (calculated for $C_{10}H_9O_2$, 161.0597). The nine unsaturated carbon signals at δ_C 194.7, 128.1, 132.7, 131.2, 121.3, 121.9, 123.0, 111.6, and 113.5 and five aromatic-hydrogen signals at δ_H 8.18 (1H, d, 2.8), 8.21 (1H, ddd, 6.6, 2.8, 1.4), 7.24–7.18 (2H, m), 7.44 (1H, dd, 6.5, 2.3), and one hydroxy-methylene at δ_H 4.72 (2H, d, 2.8), δ_C 64.9 in NMR data (Table S5) proved that compound **11** was salvinin A [43].

Compound **12** was obtained as a pale yellow powder. The molecular formula of $C_7H_7O_2N$ was determined by HR-ESI-MS (Figures S50 and S51) with the $[M - H]^-$ peak at m/z 136.0393 (calculated for $C_7H_6O_2N$, 136.0404), and $[M + H]^+$ peak at m/z 138.0554 (calculated for $C_7H_8O_2N$, 138.0550). The NMR spectra of **12** displayed six phenyl-carbon signals at δ_C 109.7, 151.2, 116.6, 135.2, 116.9, and 132.3, along with four phenyl-hydrogen signals at δ_H 6.67 (1H, dd, 7.1, 1.0), 7.30 (1H, ddd, 8.3, 7.1, 1.6), 6.66 (1H, dd, 8.3, 1.0), and 7.92 (1H, dd, 8.3, 1.6), and one carboxyl signal at δ_C 173.6 (Table S5) indicated that **12** was 2-aminobenzoic acid [44].

2.3. Antimicrobial Activities of Compounds 1–12

All the actinomycetes *Nocardia* sp. LX-1 isolated compounds (**1**–**12**) were evaluated for their antimicrobial activities. For the fermentation broth, crude extracts of the actinomycetes LX-1 displayed antimicrobial activity against *C. albicans* with the inhibition of $70 \pm 0.46\%$ at the concentration of 100 μ M. The antibacterial activities were tested against a panel of bacteria, including five phytopathogenic bacteria (*X. axonopodis*, *X. citri* pv. *malvacearum*, *D. chrysanthemi*, *P. syringae*, and *C. terrigena*), four animal pathogenic bacteria (*B. subtilis*, *E. coli*, *P. aeruginosa*, and *S. aureus*), and eight marine fouling bacteria (*A. salmonicida*, *A. hydrophila*, *E. cloacae*, *P. angustum*, *P. halotolerans*, *V. anguillarum*, *V. harveyi*, and *P. fulva*). Compounds **1**, **2**, **7**, and **10** showed antibacterial activities against *A. hydrophila* with the MIC values of 100 μ M, 100 μ M, 100 μ M, and 50 μ M, respectively. Compound **2** also exhibited antibacterial activities against *D. chrysanthemi*, *C. terrigena*, and *X. citri* pv. *malvacearum* with the MIC values of 100 μ M, 100 μ M, and 25 μ M, respectively. The MIC values of the positive control ciprofloxacin (CPFX) against *A. hydrophila*, *D. chrysanthemi*, *C. terrigena*, and *X. citri* pv. *malvacearum* were < 0.024 μ M, 0.39 μ M, 0.39 μ M, and 0.39 μ M, respectively.

The antifungal activities of the compounds **1**–**12** were also measured against one animal pathogenic fungus (*C. albicans*) and eight phytopathogenic fungi (*A. niger*, *D. citri*, *F. fujikuroi*, *F. proliferatum*, *F. oxysporum*, *F. graminearum*, *Colletotrichum* sp., and *A. alternata*). Compound **2** displayed antifungal activity against *C. albicans* with the MIC value of 100 μ M. The MIC value of the positive control CPFX against *C. albicans* was 0.20 μ M. Compound **1** showed antifungal activity against *F. fujikuroi* with the inhibition zone radius of 6.5 mm at the concentration of 100 μ M (Figure 8). Compounds **7**, **10**, and **11** exhibited antifungal activities against *D. citri*, with the inhibition zone radius of 4.7 mm, 5.3 mm, and 14 mm, respectively, at the concentration of 100 μ M (Figure 8). Prochloraz was used as the positive

control and showed an inhibition zone radius of 17 mm and 15 mm against *F. fujikuroi* and *D. citri* at the concentration of 100 μ M, respectively (Figure 8).

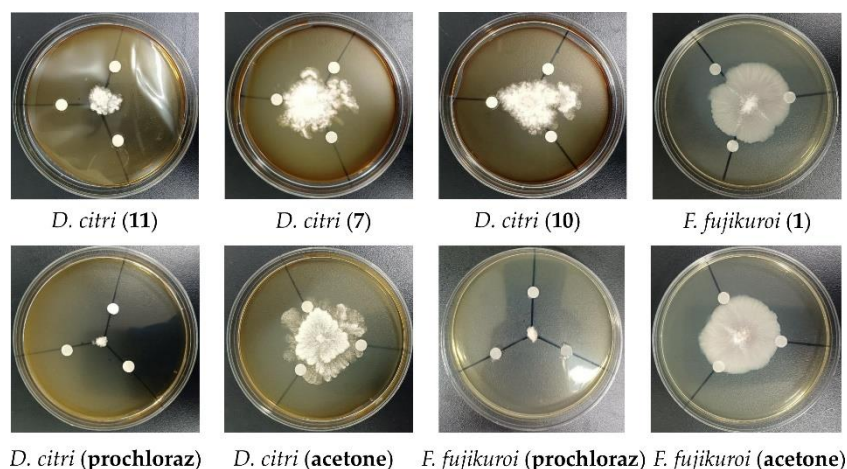


Figure 8. Antifungal activity of compounds **1**, **7**, **10**, and **11**.

3. Materials and Methods

3.1. General Experimental Procedures

The UHPLC-MS/MS spectrum was obtained on a high-resolution Q-TOF mass spectrometry Bruker impactHD (Bruker, Switzerland, Germany), combined with Ultimate3000 UHPLC (Thermo Fisher Scientific, Waltham, MA, USA). A Thermo Scientific LTQ Orbitrap XL spectrometer (Thermo Fisher Scientific, Bremen, Germany) was used to measure HR-ESI-MS. Implen GmbH NanoPhotometer N50 Touch (Implen, Munich, Germany) was used to record the UV spectrum. Nicolet 380 (Thermo Fisher, Waltham, MA, USA) was used to measure the IR spectrum. Optical rotations were measured on a JASCO P-1020 digital polarimeter (JASCO, Tokyo, Japan). NMR spectra were measured on JEOL JNM-ECZ400S (JEOL, Tokyo, Japan). The Waters 1525 system was used for HPLC purification. Silica gel (200–300 mesh) was employed for chromatographic separation. Thin-layer chromatography was recorded on precoated silica gel GF254 plates.

3.2. Actinomycetic Materials

The actinomycetes *Nocardioopsis* sp. LX-1 was isolated from the Antarctic krill *Euphausia superba* provided by Qingdao Dongfeng Ocean Fishing Co. LTD in 2019. The strain was deposited in the State Key Laboratory of Microbial Technology, Institute of Microbial Technology, Shandong University, Qingdao, China.

The identification of the actinomycetes LX-1 was determined by the analysis of the 16S rDNA gene sequence in NCBI (Nucleotide BLAST: Search nucleotide databases using a nucleotide query (nih.gov)). The 16S rDNA gene sequence of LX-1 was obtained through the polymerase chain reaction (PCR) method. The fresh actinomycetes LX-1 (about 1.00 mg) was dispersed in a 50- μ L lysis buffer (Takara, Cat# 9164) and then was saved in a metal bath (Yooning, Hangzhou, China) at 100 $^{\circ}$ C for 30 min to extract its genomic DNA as the template DNA in PCR. The PCR was conducted in a final volume of 50 μ L, which was composed of the template DNA (3 μ L), primers 27F (1 μ L) and 1492R (1 μ L), PrimeSTAR[®] Max DNA Polymerase (25 μ L, Takara, Cat# R045A), and ultrapure water (20 μ L), under the following procedures: (1) initial denaturation at 98 $^{\circ}$ C for 5 min, (2) denaturation at 98 $^{\circ}$ C for 30 s, (3) annealing at 55 $^{\circ}$ C for 30 s, (4) extension at 72 $^{\circ}$ C for 1.5 min, and (5) final extension at 72 $^{\circ}$ C for 10 min. Steps (2)–(4) were repeated 35 times. The PCR product was submitted to BGI Genomics for sequencing (BGI, Qingdao, China). The sequence of LX-1 was searched in the NCBI nucleotide collection database through the BLAST program (Nucleotide BLAST: Search nucleotide databases using a nucleotide query (nih.gov)). The actinomycetes LX-1 was identified as *Nocardioopsis* sp. whose 969 base pair 16S sequence

had 99.9% sequence identity to that of *Nocardioopsis* sp. E251 (MT533941). The sequence data have been submitted to GenBank with accession number OL687477.

3.3. Molecular Networking

3.3.1. UHPLC Parameters

The HPLC C₁₈ column (Hitachi, Tokyo, Japan, 250 mm × 4.6 mm, 5 µm) was used for liquid chromatography with the running temperature of 30 °C. Compounds were searched by UV-detector PDA with a wavelength from 190 to 400 nm, and the detection wavelengths of 210 and 254 nm were recorded to characterize the peaks. The mobile phases were MeOH (A)/H₂O (B). The elution gradient program (time (min), %A) was (0.00, 5), (5.00, 5), (60.00, 100), (75.00, 100), (80.00, 5), and (90.00, 5). The volume of the sample was 20 µL in each injection with 1.00 mL/min flow velocity.

3.3.2. MS/MS Parameters

MS/MS analyses were performed by high-resolution Q-TOF mass spectrometry by using a Bruker impactHD. The ESI source parameters were set as follows: capillary source voltage at 3500 V, positive-ion mode, drying-gas temperature at 200 °C, drying-gas flow rate at 4 L/min, and end plate offset voltage at 500 V. MS scans were recorded in full scan mode with a range of *m/z* 50–1500 (100 ms scan time), and the mass resolution was 40,000 at *m/z* 1222.

3.3.3. Molecular Network Analysis

The molecular network was formed by GNPS workflow (<http://gnps.ucsd.edu>, accessed on 29 November 2021) [18]. Bruker Daltonics was used to convert the UHPLC-MS/MS raw data file into .mzXML. The parameter settings of the molecular network were detailed in our previous research [22,23]. The results were visualized by using the software package Cytoscape 3.8.0 (Download from <https://cytoscape.org/>).

3.4. Extraction and Isolation

The actinomycetes *Nocardioopsis* sp. LX-1 was cultured in a NB liquid medium in 100 Erlenmeyer flasks (200 mL in each 500 mL flask) at 20 °C for 45 days. The mycelia were filtered from the broth by two layers of gauze. Then, the mycelia were first extracted by ethyl acetate (EA) three times (3 × 200 mL) and then with dichloromethane (DCM)/methanol (MA) (*v/v*, 1:1) three times (3 × 200 mL). The c broth was obtained through repeated extraction with EA (3 × 20 L). All of the fungal crude extracts were put together and evaporated to dryness under reduced pressure to provide a residue (2.2 g). The residue was subjected to silica gel column chromatography (CC) eluted with EA–petroleum ether (PE) (0–100%) and MA–EA (0–100%) to obtain four fractions (Fr.1–Fr.4). Fr.2 was the pure compound **12** (70.5 mg). Fr.3 was separated through CC on silica gel eluted with EA–PE (0–50%) to give three fractions (Fr.3.1–Fr.3.3). Fr.3.2 was purified by using semipreparative HPLC on an ODS column (Kromasil C₁₈, 250 × 10 mm, 5 µm, 2 mL/min) eluted with 50% MA–H₂O to give compounds **2** (1.3 mg) and **9** (1.0 mg). Fr.3.3 was separated on HPLC eluted with 45% MA–H₂O for **11** (1.9 mg). Fr.4 was separated through CC on silica gel eluted with EA–PE (30–90%) to afford three fractions (Fr.4.1–Fr.4.3). Fr.4.2 was subjected on HPLC with 35% MA–H₂O for **3** (17.4 mg), **4** (17.9 mg), **6** (19.9 mg), and **10** (4.2 mg). Fr.4.3 was separated by HPLC eluted with 30% MA–H₂O to give four fractions (Fr.4.3.1–Fr.4.3.4). Fr.4.3.4 was the pure compound **7** (44.4 mg). Fr.4.3.2 was further purified through HPLC eluted with 25% MA–H₂O for **8** (36.8 mg). Fr.4.3.3 was further purified through HPLC eluted with 25% MA–H₂O for **1** (1.6 mg) and **5** (13.6 mg). The details are as follows.

Nocarpyrroline A (**1**): amorphous white powder; UV (CH₃OH) λ_{max} (log ε): 288 (2.85); [α]_D²⁰ –129.13° (c 0.033, MeOH); ¹H and ¹³C NMR data (see Table 2); HR-ESI-MS *m/z* [M – H][–] 257.0939 (calculated for C₁₄H₁₃O₃N₂, 257.0932) and [M + H]⁺ peak at *m/z* 259.1080 (calculated for C₁₄H₁₅O₃N₂, 259.1077).

Daidzene (**2**): amorphous white powder; ^1H and ^{13}C NMR data (see Table S1); HR-ESI-MS m/z $[\text{M} - \text{H}]^-$ 253.0501 (calculated for $\text{C}_{15}\text{H}_9\text{O}_4$, 253.0506) and $[\text{M} + \text{H}]^+$ 255.0660 (calculated for $\text{C}_{15}\text{H}_{11}\text{O}_4$, 255.0652).

Cyclo(D-Pro-L-Val) (**3**): amorphous white powder; ^1H and ^{13}C NMR data (see Tables S2 and S3); specific OR data (see Table S4); HR-ESI-MS m/z $[\text{M} - \text{H}]^-$ 195.1130 (calculated for $\text{C}_{10}\text{H}_{15}\text{O}_2\text{N}_2$, 195.1139) and $[\text{M} + \text{H}]^+$ 197.1294 (calculated for $\text{C}_{10}\text{H}_{17}\text{O}_2\text{N}_2$, 197.1285).

Cyclo(4-methyl-D-Pro-L-Nva) (**4**): amorphous white powder; ^1H and ^{13}C NMR data (see Tables S2 and S3); specific OR data (see Table S4); HR-ESI-MS m/z $[\text{M} - \text{H}]^-$ 209.1288 (calculated for $\text{C}_{11}\text{H}_{17}\text{O}_2\text{N}_2$, 209.1296) and $[\text{M} + \text{H}]^+$ 211.1449 (calculated for $\text{C}_{11}\text{H}_{19}\text{O}_2\text{N}_2$, 211.1441).

Cyclo(*trans*-4-OH-L-Pro-L-Phe) (**5**): colorless oil; ^1H and ^{13}C NMR data (see Tables S2 and S3); specific OR data (see Table S4); HR-ESI-MS m/z $[\text{M} - \text{H}]^-$ 259.1083 (calculated for $\text{C}_{14}\text{H}_{15}\text{O}_3\text{N}_2$, 259.1088), and $[\text{M} + \text{H}]^+$ 261.1244 (calculated for $\text{C}_{14}\text{H}_{17}\text{O}_3\text{N}_2$, 261.1234) and 283.1063 (calculated for $\text{C}_{14}\text{H}_{16}\text{O}_3\text{N}_2\text{Na}$, 283.1053).

Cyclo(L-Pro-L-Phe) (**6**): colorless oil; ^1H and ^{13}C NMR data (see Tables S2 and S3); specific OR data (see Table S4); HR-ESI-MS m/z $[\text{M} - \text{H}]^-$ 243.1133 (calculated for $\text{C}_{14}\text{H}_{15}\text{O}_2\text{N}_2$, 243.1139), and $[\text{M} + \text{H}]^+$ 245.1294 (calculated for $\text{C}_{14}\text{H}_{17}\text{O}_2\text{N}_2$, 245.1285).

Cyclo(D-Pro-L-Phe) (**7**): colorless oil; ^1H and ^{13}C NMR data (see Tables S2 and S3); specific OR data (see Table S4); HR-ESI-MS m/z $[\text{M} - \text{H}]^-$ 243.1133 (calculated for $\text{C}_{14}\text{H}_{15}\text{O}_2\text{N}_2$, 243.1139), and $[\text{M} + \text{H}]^+$ 245.1293 (calculated for $\text{C}_{14}\text{H}_{17}\text{O}_2\text{N}_2$, 245.1285) and 267.1112 (calculated for $\text{C}_{14}\text{H}_{16}\text{O}_2\text{N}_2\text{Na}$, 267.1104).

Cyclo(4-hydroxyl-L-Pro-L-Leu) (**8**): amorphous white powder; ^1H and ^{13}C NMR data (see Tables S2 and S3); specific OR data (see Table S4); HR-ESI-MS m/z $[\text{M} - \text{H}]^-$ 225.1238 (calculated for $\text{C}_{11}\text{H}_{17}\text{O}_3\text{N}_2$, 225.1245), and $[\text{M} + \text{H}]^+$ 227.1398 (calculated for $\text{C}_{11}\text{H}_{19}\text{O}_3\text{N}_2$, 227.1390) and 249.1217 (calculated for $\text{C}_{11}\text{H}_{18}\text{O}_3\text{N}_2\text{Na}$, 249.1210).

2,4(1*H*, 3*H*)Quinazolinedione (**9**): amorphous white powder; ^1H and ^{13}C NMR data (see Table S5); HR-ESI-MS m/z $[\text{M} - \text{H}]^-$ 161.0345 (calculated for $\text{C}_8\text{H}_5\text{O}_2\text{N}_2$, 161.0357).

Uracil (**10**): colorless needles; ^1H and ^{13}C NMR data (see Table S5); HR-ESI-MS m/z $[\text{M} - \text{H}]^-$ 111.0187 (calculated for $\text{C}_4\text{H}_3\text{O}_2\text{N}_2$, 111.0200), and $[\text{M} + \text{H}]^+$ 113.0351 (calculated for $\text{C}_4\text{H}_5\text{O}_2\text{N}_2$, 113.0346).

Salvinin A (**11**): pale yellow powder; ^1H and ^{13}C NMR data (see Table S5); HR-APCI-MS m/z $[\text{M} + \text{H}]^+$ 161.0602 (calculated for $\text{C}_{10}\text{H}_9\text{O}_2$, 161.0597).

2-Aminobenzoic acid (**12**): pale yellow powder; ^1H and ^{13}C NMR data (see Table S5); HR-ESI-MS m/z $[\text{M} - \text{H}]^-$ 136.0393 (calculated for $\text{C}_7\text{H}_6\text{O}_2\text{N}$, 136.0404), and $[\text{M} + \text{H}]^+$ 138.0554 (calculated for $\text{C}_7\text{H}_8\text{O}_2\text{N}$, 138.0550).

3.5. Antibacterial Activity Assay

The antibacterial activities were evaluated by the conventional broth dilution assay [45]. Five phytopathogenic bacteria (*Xanthomonas citri* *pv.* *malvacearum*, *X. axonopodis*, *Comamonas terrigena*, *Pseudomonas syringae*, and *Dickeya chrysanthemi*), four animal pathogenic bacteria (*Escherichia coli*, *P. aeruginosa*, *Staphylococcus aureus*, and *Bacillus subtilis*), and eight marine fouling bacteria (*Aeromonas hydrophila*, *A. salmonicida*, *Enterobacter cloacae*, *P. fulva*, *Vibrio anguillarum*, *V. harveyi*, *Photobacterium halotolerans*, and *P. angustum*) were used, and ciprofloxacin (CPFX) and DMSO were used as the positive and negative control, respectively. The antibacterial activity assay was carried out by using previously described methods [22,23]. The tested concentrations of isolated compounds and CPFX were 100 μM , 50 μM , 25 μM , 12.5 μM , 6.25 μM , 3.13 μM , 1.56 μM , 0.78 μM , 0.39 μM , and 100 μM , 50 μM , 25 μM , 12.5 μM , 6.25 μM , 3.13 μM , 1.56 μM , 0.78 μM , 0.39 μM , 0.20 μM , 0.10 μM , 0.049 μM , and 0.024 μM , respectively.

3.6. Antifungal Activity Assay

The antifungal activity against *Candida albicans* was evaluated through the conventional broth dilution method [45]. CPFX and DMSO were used as the positive and negative

control, respectively. The antifungal activities against eight phytopathogenic fungi, *Aspergillus niger*, *Alternaria alternata*, *Diaporthe citri*, *Fusarium fujikuroi*, *F. oxysporum*, *F. graminearum*, *F. proliferatum*, and *Colletotrichum* sp., were assessed through the modified agar diffusion test method [46]. The isolated compounds to be tested were dissolved in acetone at a final concentration of 100 μ M. The compound solving solution was transferred to a sterile filter disk (diameter 6 mm, each 20 μ L), which was placed on the agar growth medium for the tested fungi. Prochloraz was used as the positive control with the test concentration of 100 μ M. Acetone was used as negative control.

4. Conclusions

In summary, 16 compounds **a–p** were recognized from the metabolites of Antarctic krill (*E. superba*)-derived actinomycetes *Nocardiopsis* sp. LX-1 by the method of molecular networking. One new pyrroline, nocarpyrroline A (**1**), along with 11 known compounds **2–12**, were isolated from the actinomycetes *Nocardiopsis* sp. LX-1 according to the molecular networking analysis. Among them, compound **2** was the same as the molecular networking investigated isoflavonoid **e**, and this is the first time isoflavonoid from the genus *Nocardiopsis* has been isolated. New compound **1** showed antibacterial activity against *A. hydrophila*, and antifungal activity against *F. fujikuroi*. Compound **2** exhibited broad-spectrum antibacterial activities against *A. hydrophila*, *D. chrysanthemi*, *C. terrigena*, and *X. citri* pv. *malvacearum*, and antifungal activity against *C. albicans*. Compounds **7** and **10** displayed antibacterial activities against *A. hydrophila*, and **7**, **10**, and **11** revealed antifungal activities against *D. citri*. None of the annotated compounds **a–p** by the method of molecular networking had been isolated from the genus *Nocardiopsis*. Nocarpyrroline A (**1**), features an unprecedented 4,5-dihydro-pyrrole-2-carbonitrile substructure, and it is the first pyrroline discovered from the genus *Nocardiopsis*. This study further demonstrated the potential of Antarctic microbes to produce new bioactive natural products and proved the significance of molecular networking in the research of microbial secondary metabolites.

The extremely cold, arid, and fierce solar radiational environments of Antarctica, have created a unique ecological system containing abundant microbial resources with the ability to produce structurally specific active substances. Antarctic krill, as the foundation of the Antarctic marine ecosystem, contain rich symbiotic or parasitical microorganisms that produce special secondary metabolites. Few research papers have studied Antarctic krill-derived microorganisms and their secondary metabolites until now. More attention should be paid to chemical investigation and bioactive evaluation of the natural products isolated from Antarctic krill-derived microorganisms, which could find new bioactive compounds to provide the structural basis for new drug development.

Supplementary Materials: The following supporting information can be downloaded at: <https://www.mdpi.com/article/10.3390/md21020127/s1>, Figures S1–S51: NMR, MS, and IR spectra of compounds **1–12**; Figures S52–S68: MS/MS spectra of compounds **a–p** (black) compared with GNPS library spectra (green); Tables S1–S3 and Table S5: NMR data of compounds **2–12**; Table S4: Specific OR of cyclic dipeptides **3–8** in MeOH.

Author Contributions: Conceptualization, T.S.; methodology, T.S. and Y.-J.L.; software, T.S.; validation, Y.-J.L., D.-Y.S. and B.W.; formal analysis, T.S. and Y.-F.W.; investigation, T.S. and Z.-M.W.; resources, D.-Y.S. and Y.-F.W.; data curation, T.S.; writing—original draft preparation, T.S.; writing—review and editing, T.S.; visualization, Z.-M.W.; supervision, D.-Y.S. and B.W.; project administration, D.-Y.S. and B.W.; funding acquisition, T.S., D.-Y.S. and B.W. All authors have read and agreed to the published version of the manuscript.

Funding: This work was supported by the Shandong Provincial Natural Science Foundation (No. ZR2020QD111); the National Natural Science Foundation of China (No. 82104029; 21868011; 82003787); and supported by the Talent Support Program of Shandong University of Science and Technology; and the Top-notch Young Professionals.

Institutional Review Board Statement: Not applicable.

Informed Consent Statement: Not applicable.

Data Availability Statement: The datasets presented in this study can be found in online repositories. The names of the repository/repositories and accession number can be found below: <https://www.ncbi.nlm.nih.gov/nuccore/OL687477.1/>, accessed on 7 December 2021. The molecular network of the secondary metabolic profile of the actinomycetes *Nocardiopsis* sp. LX-1 can be found in <https://gnps.ucsd.edu/ProteoSAFe/status.jsp?task=37dd96194c924f6d9daee62672ba930>, assessed on 29 November 2021.

Acknowledgments: We would like to thank the Qingdao Dongfeng Ocean Fishing Co. LTD for supporting sample; Zheng-kun Du in NMR measuring from Aluminum Battery Research Center, College of Energy Storage Technology of Shandong University of Science and Technology; Jing-Yao Qu, Jing Zhu, Guan-Nan Lin, and Zhi-Feng Li in MS, Hai-Yan Sui in NMR for help and guidance from the State Key laboratory of Microbial Technology of Shandong University.

Conflicts of Interest: The authors declare no conflict of interest.

References

- Shi, T.; Li, X.-Q.; Zheng, L.; Zhang, Y.-H.; Dai, J.-J.; Shang, E.-L.; Yu, Y.-Y.; Zhang, Y.-T.; Hu, W.-P.; Shi, D.-Y. Sesquiterpenoids from the Antarctic fungus *Pseudogymnoascus* sp. HSX2#-11. *Front. Microbiol.* **2021**, *12*, 688202. [CrossRef] [PubMed]
- Colletti, A.; Cravotto, G.; Citi, V.; Martelli, A.; Testai, L.; Cicero, A.F. Advances in technologies for highly active omega-3 fatty acids from krill oil: Clinical applications. *Mar. Drugs* **2021**, *19*, 306. [CrossRef] [PubMed]
- Manno, C.; Fielding, S.; Stowasser, G.; Murphy, E.; Thorpe, S.; Tarling, G. Continuous moulting by Antarctic krill drives major pulses of carbon export in the north Scotia Sea, Southern Ocean. *Nat. Commun.* **2020**, *11*, 6051. [CrossRef] [PubMed]
- Huang, Y.; Bian, C.; Liu, Z.; Wang, L.; Xue, C.; Huang, H.; Yi, Y.; You, X.; Song, W.; Mao, X. The first genome survey of the Antarctic Krill (*Euphausia superba*) provides a valuable genetic resource for polar biomedical research. *Mar. Drugs* **2020**, *18*, 185. [CrossRef] [PubMed]
- Nicol, S.; Foster, J.; Kawaguchi, S. The fishery for Antarctic krill—Recent developments. *Fish Fish.* **2012**, *13*, 30–40. [CrossRef]
- Bengtson Nash, S.M.; Schlabach, M.; Nichols, P.D. A nutritional-toxicological assessment of Antarctic krill oil versus fish oil dietary supplements. *Nutrients* **2014**, *6*, 3382–3402. [CrossRef]
- Warwick-Evans, V.; Fielding, S.; Reiss, C.; Watters, G.; Trathan, P.N. Estimating the average distribution of Antarctic krill *Euphausia superba* at the northern Antarctic Peninsula during austral summer and winter. *Polar Biol.* **2022**, *45*, 857–871. [CrossRef]
- Cui, X.; Zhu, G.; Liu, H.; Jiang, G.; Wang, Y.; Zhu, W. Diversity and function of the Antarctic krill microorganisms from *Euphausia superba*. *Sci. Rep.* **2016**, *6*, 36496. [CrossRef]
- Yang, Q. Taxonomic identification and bioactivity screening of the symbiotic bacteria strains of *Euphausia superba* from Antarctic ocean. *Appl. Mech. Mater.* **2013**, 295–298, 173–177. [CrossRef]
- Zheng, L.; Liang, F.; Zhu, M.; Kang, D.; Zhu, X.; Yuan, Z. *Euphausia superba* Symbiotic Bacteria *Psychrobacter* sp. NL-6, *Euphausia superba* Antioxidant Peptide, Its Preparation Method and Application. China Patent Application No. CN106244484A, 21 December 2016.
- Patel, G.B.; Rakholiya, P.; Shindhal, T.; Varjani, S.; Tabhani, N.; Shah, K.R. Lipolytic *Nocardiopsis* for reduction of pollution load in textile industry effluent and SWISS model for structural study of lipase. *Bioresour. Technol.* **2021**, *341*, 125673. [CrossRef]
- Patel, K.B.; Thakker, J.N. Growth promotion and biocontrol activity of *Nocardiopsis dassonvillei* strain YM12: An isolate from coastal agricultural land of Khamhat. *Vegetos* **2019**, *32*, 571–582. [CrossRef]
- Sivaperumal, P.; Kamala, K.; Rajaram, R. Adsorption of cesium ion by marine actinobacterium *Nocardiopsis* sp. ¹³H and their extracellular polymeric substances (EPS) role in bioremediation. *Environ. Sci. Pollut. Res.* **2018**, *25*, 4254–4267. [CrossRef]
- Bennur, T.; Ravi Kumar, A.; Zinjarde, S.; Javdekar, V. *Nocardiopsis* species: A potential source of bioactive compounds. *J. Appl. Microbiol.* **2016**, *120*, 1–16. [CrossRef]
- Ibrahim, A.H.; Desoukey, S.Y.; Fouad, M.A.; Kamel, M.S.; Gulder, T.A.; Abdelmohsen, U.R. Natural product potential of the genus *Nocardiopsis*. *Mar. Drugs* **2018**, *16*, 147. [CrossRef]
- Shi, T.; Wang, Y.-F.; Wang, H.; Wang, B. Genus *Nocardiopsis*: A Prolific Producer of Natural Products. *Mar. Drugs* **2022**, *20*, 374. [CrossRef]
- Zhang, J.W.; Zeng, R.Y. Psychrotrophic amylolytic bacteria from deep sea sediment of Prydz Bay, Antarctic: Diversity and characterization of amylases. *World J. Microbiol. Biotechnol.* **2007**, *23*, 1551–1557. [CrossRef]
- Wang, M.; Carver, J.J.; Phelan, V.V.; Sanchez, L.M.; Garg, N.; Peng, Y.; Nguyen, D.D.; Watrous, J.; Kapon, C.A.; Luzzatto-Knaan, T. Sharing and community curation of mass spectrometry data with Global Natural Products Social Molecular Networking. *Nat. Biotechnol.* **2016**, *34*, 828–837. [CrossRef]
- Quinn, R.A.; Nothias, L.-F.; Vining, O.; Meehan, M.; Esquenazi, E.; Dorrestein, P.C. Molecular networking as a drug discovery, drug metabolism, and precision medicine strategy. *Trends Pharmacol. Sci.* **2017**, *38*, 143–154. [CrossRef]
- Nothias, L.-F.; Petras, D.; Schmid, R.; Dührkop, K.; Rainer, J.; Sarvepalli, A.; Protzyuk, I.; Ernst, M.; Tsugawa, H.; Fleischauer, M. Feature-based molecular networking in the GNPS analysis environment. *Nat. Methods* **2020**, *17*, 905–908. [CrossRef]

21. Yang, J.Y.; Sanchez, L.M.; Rath, C.M.; Liu, X.; Boudreau, P.D.; Bruns, N.; Glukhov, E.; Wodtke, A.; De Felicio, R.; Fenner, A. Molecular networking as a dereplication strategy. *J. Nat. Prod.* **2013**, *76*, 1686–1699. [\[CrossRef\]](#)
22. Shi, T.; Yu, Y.Y.; Dai, J.J.; Zhang, Y.T.; Shi, D.Y. New polyketides from the Antarctic fungus *Pseudogymnoascus* sp. HSX2#-11. *Mar. Drugs* **2021**, *19*, 168. [\[PubMed\]](#)
23. Shi, T.; Li, X.-Q.; Wang, Z.-M.; Zheng, L.; Yu, Y.-Y.; Dai, J.-J.; Shi, D.-Y. Bioactivity-guided screening of antimicrobial secondary metabolites from Antarctic cultivable fungus *Acrostalagmus luteoalbus* CH-6 combined with molecular networking. *Mar. Drugs* **2022**, *20*, 334. [\[CrossRef\]](#) [\[PubMed\]](#)
24. Monowar, T.; Rahman, M.S.; Bhore, S.J.; Sathasivam, K.V. Endophytic bacteria *Enterobacter hormaechei* fabricated silver nanoparticles and their antimicrobial activity. *Pharmaceutics* **2021**, *13*, 511. [\[CrossRef\]](#) [\[PubMed\]](#)
25. Morrison, L.; Zembower, T.R. Antimicrobial resistance. *Gastrointest. Endosc. Clin.* **2020**, *30*, 619–635. [\[CrossRef\]](#) [\[PubMed\]](#)
26. Hofer, U. The cost of antimicrobial resistance. *Nat. Rev. Microbiol.* **2019**, *17*, 3. [\[CrossRef\]](#)
27. WHO. *World Health Statistics 2022: Monitoring Health for the SDGs, Sustainable Development Goals*; WHO: Geneva, Switzerland, 2022; ISBN 9789240051157.
28. Butler, M.S.; Buss, A.D. Natural products—the future scaffolds for novel antibiotics? *Biochem. Pharmacol.* **2006**, *71*, 919–929. [\[CrossRef\]](#)
29. Mu, W.; Yu, S.; Zhu, L.; Zhang, T.; Jiang, B. Recent research on 3-phenyllactic acid, a broad-spectrum antimicrobial compound. *Appl. Microbiol. Biot.* **2012**, *95*, 1155–1163. [\[CrossRef\]](#)
30. Alcázar Magaña, A.; Kamimura, N.; Soumyanath, A.; Stevens, J.F.; Maier, C.S. Caffeoylquinic acids: Chemistry, biosynthesis, occurrence, analytical challenges, and bioactivity. *Plant J.* **2021**, *107*, 1299–1319. [\[CrossRef\]](#)
31. Bogner, A.N.; Stiers, K.M.; Tanner, J.J. Structure, biochemistry, and gene expression patterns of the proline biosynthetic enzyme pyrroline-5-carboxylate reductase (PYCR), an emerging cancer therapy target. *Amino Acids* **2021**, *53*, 1817–1834. [\[CrossRef\]](#)
32. Hofman, G.-J.; Ottoy, E.; Light, M.E.; Kieffer, B.; Martins, J.C.; Kuprov, I.; Sinnaeve, D.; Linclau, B. Synthesis and conformational properties of 3,4-difluoro-L-prolines. *J. Org. Chem.* **2019**, *84*, 3100–3120. [\[CrossRef\]](#)
33. Burgemeister, T.; Dannhardt, G.; Mach-Bindl, M.; Noeth, H. Reactions of 1-pyrrolines with ketenes-carbapenams, N-acyl-2-pyrrolines, and ω -(acylamino) ketones. *ChemInform* **1988**, *112*, 93. [\[CrossRef\]](#)
34. Xu, D.; Jiang, H.; Pang, Z.; Pan, F. Extraction, isolation of isoflavones in tempeh and their chemical structure determination. *Food Ferment. Ind.* **2001**, *27*, 1–4.
35. Zeng, X.R.; Jiao, W.H.; Tang, J.S.; Gao, H.; Hong, K.; Jia, L.I.; Yao, X.S. Secondary metabolites from marine actinomycete *Streptomyces* sp. (No.30701). *Chin. J. Med. Chem.* **2010**, *20*, 298–303.
36. Adamczeski, M.; Reed, A.R.; Crews, P. New and known diketopiperazines from the Caribbean sponge, *Calyx* cf. *podatypa*. *J. Nat. Prod.* **1995**, *58*, 201–208. [\[CrossRef\]](#)
37. Xiang, W.-X.; Liu, Q.; Li, X.-M.; Lu, C.-H.; Shen, Y.-M. Four pairs of proline-containing cyclic dipeptides from *Nocardiopsis* sp. HT88, an endophytic bacterium of *Mallotus nudiflorus* L. *Nat. Prod. Res.* **2020**, *34*, 2219–2224. [\[CrossRef\]](#)
38. Martinez-Luis, S.; Ballesteros, J.; Gutierrez, M. Antibacterial constituents from the octocoral-associated bacterium *Pseudoalteromonas* sp. *Rev. Latinoam. Quim.* **2011**, *39*, 75–83.
39. Wang, G.; Dai, S.; Chen, M.; Wu, H.; Xie, L.; Luo, X.; Li, X. Two diketopiperazine cyclo(Pro-Phe) isomers from marine bacterium *Bacillus subtilis* sp. 13-2. *Chem. Nat. Compd.* **2010**, *46*, 583–585. [\[CrossRef\]](#)
40. Cronan Jr, J.M.; Davidson, T.R.; Singleton, F.L.; Colwell, R.R.; Cardellina, J.H. Plant growth promoters isolated from a marine bacterium associated with *Palythoa* sp. *Nat. Prod. Lett.* **1998**, *11*, 271–278. [\[CrossRef\]](#)
41. Li, L.; Liang, H.Q.; Liao, S.X.; Qiao, C.Z.; Yang, G.J.; Dong, T.Y. Chemical studies of *Strobilanthes cusia*. *Acta Pharm. Sin.* **1993**, *28*, 238–240.
42. Ding, Z.G.; Zhao, J.Y.; Yang, P.W.; Li, M.G.; Huang, R.; Cui, X.L.; Wen, M.L. ^1H and ^{13}C NMR assignments of eight nitrogen containing compounds from *Nocardia alba* sp. nov. (YIM 30243T). *Magn. Reson. Chem.* **2009**, *47*, 366–370. [\[CrossRef\]](#)
43. Li, S.; Wang, P.; Deng, G.; Yuan, W.; Su, Z. Cytotoxic compounds from invasive giant salvinia (*Salvinia molesta*) against human tumor cells. *Bioorg. Med. Chem. Lett.* **2013**, *23*, 6682–6687. [\[CrossRef\]](#) [\[PubMed\]](#)
44. Regulska, E.; Samsonowicz, M.; Świsłocka, R.; Lewandowski, W. Theoretical and experimental study of alkali metal *o*-, *m*- and *p*-aminobenzoates in comparison with nitrobenzoates. *J. Mol. Struct.* **2009**, *936*, 162–170. [\[CrossRef\]](#)
45. Appendino, G.; Gibbons, S.; Giana, A.; Pagani, A.; Grassi, G.; Stavri, M.; Smith, E.; Rahman, M.M. Antibacterial cannabinoids from *Cannabis sativa*: A structure-activity study. *J. Nat. Prod.* **2008**, *71*, 1427–1430. [\[CrossRef\]](#) [\[PubMed\]](#)
46. Zhao, D.-L.; Wang, H.-S.; Gao, L.-W.; Zhang, P. Tennesenoid A, an unprecedented steroid-sorbicillinoid adduct from the marine-derived endophyte of *Aspergillus* sp. strain 1022LEF. *Front. Mar. Sci.* **2022**, *9*, 816. [\[CrossRef\]](#)

Disclaimer/Publisher’s Note: The statements, opinions and data contained in all publications are solely those of the individual author(s) and contributor(s) and not of MDPI and/or the editor(s). MDPI and/or the editor(s) disclaim responsibility for any injury to people or property resulting from any ideas, methods, instructions or products referred to in the content.